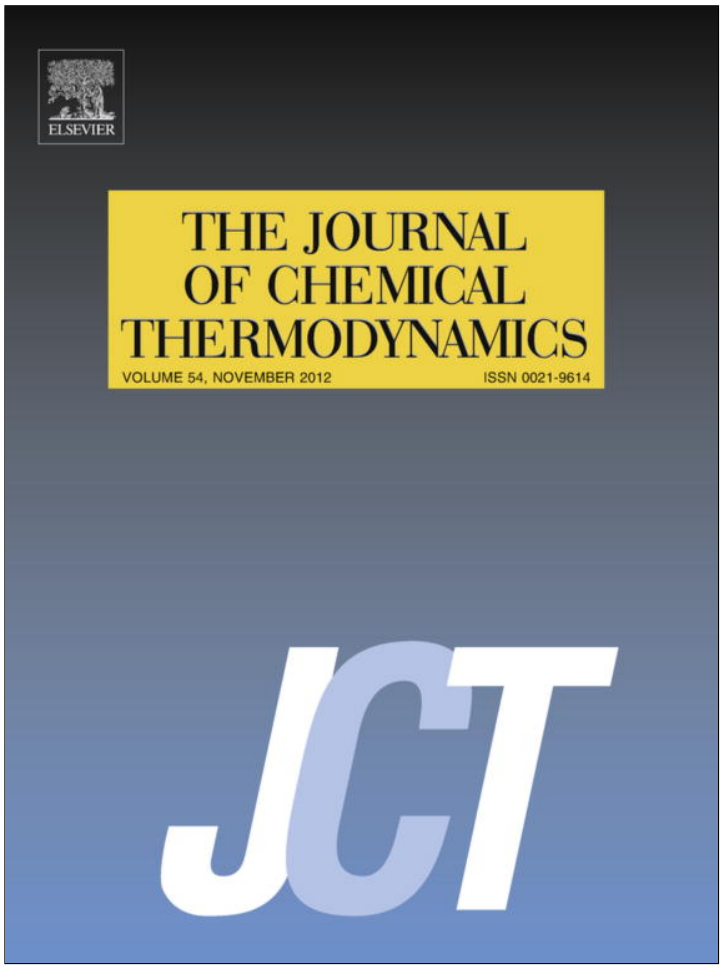

J. Chem. Thermodynamics 54 (2012) 421–428

Contents lists available at SciVerse ScienceDirect

J. Chem. Thermodynamics

journal homepage: www.elsevier.com/locate/jct

Drug–DNA binding thermodynamics: A comparative study of aristololactam-β-D-glucoside and daunomycin

Abhi Das, Gopinatha Suresh Kumar *

Biophysical Chemistry Laboratory, Chemistry Division, CSIR – Indian Institute of Chemical Biology, Kolkata 700 032, India

ARTICLE INFO

Article history:
Received 24 April 2012
Received in revised form 16 May 2012
Accepted 22 May 2012
Available online 30 May 2012

Keywords:
Aristololactam-β-D-glucoside
Daunomycin
DNA binding
Thermodynamics

ABSTRACT

Thermal melting and microcalorimetric studies have been carried out to investigate and compare the thermodynamics of interaction of two sugars bearing drugs *viz.* the aristololactam-β-D-glucoside (ADG) and daunomycin (DAU) with DNA. Both compounds stabilized DNA against thermal strand separation but daunomycin promoted a much higher stability compared to ADG. The binding affinity of ADG was of the order of $10^5\ M^{-1}$ while that of daunomycin was higher by one order ($10^6\ M^{-1}$). There is only one class of binding site on DNA for both ADG and DAU. The binding was predominantly enthalpy driven for both compounds but the entropy contribution was different. Although higher salt concentration decreased the binding affinity in both cases the variation was higher for DAU compared to ADG. Temperature dependent calorimetric data suggested that the enthalpy and entropy changes reduced but compensated each other to keep the Gibbs free energy change almost same and gave negative ΔC_p° values. The complexation of both drugs to DNA appears to be similar with higher affinity for DAU over ADG but the energetics are different. DAU is a better DNA intercalator compared to ADG.

1. Introduction

Interaction of small molecules with nucleic acids continues to arouse significant interest in researchers in terms of elucidating the various aspects of the binding for development of potential DNA targeted therapeutics [1–4]. In particular, the energetics of the interaction is an important aspect that is now receiving great attention in order to correlate with the structural data for efficient drug design and development [5,6]. Aristololactam-β-D-glucoside (ADG) (figure 1A) is an alkaloid of the aristolochia group that has attracted recent attention for extensive biological activities [7,8]. ADG has close similarity to the anthracycline antibiotic daunomycin (DAU) with the daunosamine sugar moiety (figure 1B), which is a potent anticancer drug currently used in clinics [9–12]. Emerging from DAU some thousand new anthracycline analogs were synthesized in search of stronger biological activity and lower toxicity [13–16]. A common feature of ADG and DAU is the DNA intercalative binding [10,17–19]. X-ray studies of daunomycin-DNA complex have revealed that the sugar moiety lies in the minor groove making favourable polyelectrolytic contributions to the Gibbs energy [20,21]. But for ADG, in the absence of a DNA complexed crystal structure, no such clear cut evidences are available in respect of the specific role of the sugar moiety in the binding. Maiti and coworkers have reported that ADG binding is GC base pair specific [19] and sensitive to sodium ion concentrations [22]. But a detailed thermodynamic analysis on the interaction of ADG with DNA in comparison with DAU is still lacking and the molecular aspects of the role of sugar moiety if any in the energetics of its interaction are not clear. To understand the energetics of the interaction of ADG binding to DNA and to provide a detailed thermodynamic basis for the binding of ADG in comparison with DAU calorimetric studies were performed in conjunction with optical thermal melting experiments. In this paper we report the comparative thermodynamics of the interaction of ADG and DAU with DNA.

2. Experimental

2.1. Materials

Deoxyribonucleic acid sodium salt from herring testes, type XIV (HT DNA 41.2% GC content), and daunomycin hydrochloride (>90%) were obtained from Sigma–Aldrich Corporation (St. Louis, MO, USA). Aristololactam-β-D-glucoside was extracted from *Aristolochia indica* and crystallized twice from ethanol and was provided by Dr. Basudeb Achari, Ex. Scientist of the Chemistry Division of our institute. Its purity (>99%) was checked by various physicochemical techniques in our laboratory as reported earlier [23,24]. Buffer salts and other reagents were from Sigma–Aldrich. All chemicals and reagents were of analytical grade or better and used as received.

* Corresponding author. Address: Biophysical Chemistry Laboratory, CSIR – Indian Institute of Chemical Biology, 4, Raja S.C. Mullick Road, Jadavpur, Kolkata 700 032, India. Tel.: +91 33 2472 4049/2499 5723; fax: +91 33 2472 3967.
E-mail addresses: gskumar@iicb.res.in, gskumar@csiriicb.in (G. Suresh Kumar).

0021-9614/$ - see front matter © 2012 Elsevier Ltd. All rights reserved.
http://dx.doi.org/10.1016/j.jct.2012.05.028

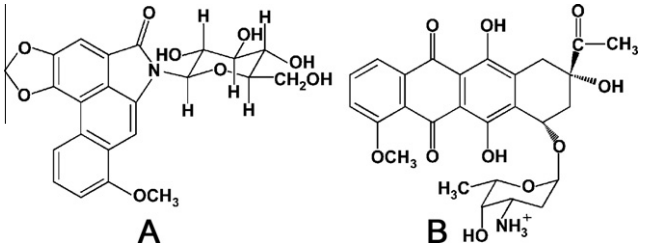

FIGURE 1. Chemical structure of (A) aristololactam-β-D-glucoside and (B) daunomycin.

Deionised and triple distilled water that was passed through Millipore filters of pore size 0.22 μM (Millipore India Pvt. Ltd. Bangalore, India) was used for preparing buffer solutions.

2.2. Preparation of DNA, ADG, and DAU solutions

The DNA sample was sonicated in a Labsonic sonicator (B. Brown, Germany) to molar mass of (1 to $2 \cdot 10^5$) Da and dialyzed under sterile conditions. Stock solutions of sonicated DNA and DAU were prepared in the experimental buffer, 20 mM citrate–phosphate (CP) buffer containing 10 mM Na_2HPO_4 and 0.425 mM citric acid, pH 7.01. The ratio of absorbance at 260 nm to 280 nm for the DNA solution was around 1.82 indicating the protein free nature of the sample. DNA concentration was determined spectrophotometrically using a molar extinction coefficient (ε) of 13,200 $M^{-1} \cdot cm^{-1}$ at 260 nm and expressed as molarity of base pairs. For preparation of ADG solutions for binding studies, CP buffer containing additionally 240 mM of DMSO was used [17,19]. The concentration of DAU and ADG were determined by absorbance measurements using molar extinction coefficients (ε as follows: ADG – 10,930 $M^{-1} \cdot cm^{-1}$ at 398 nm (in DMSO) and DAU – 11,500 $M^{-1} \cdot cm^{-1}$ at 480 nm (in buffer), respectively [19,25]. ADG and DAU solutions were kept protected in the dark and obeyed Beers' law in the concentration range used in this study.

2.3. Absorption spectroscopy

A Jasco V660 double beam double monochromator spectrophotometer (Jasco International Co., Hachioji, Japan) was used for absorption spectral measurements employing matched 1 cm path length matched quartz cuvettes. Sample temperature was controlled by a Lab companion water bath.

2.4. Optical thermal melting studies

Absorbance *versus* temperature curves (melting profiles) of DNA and DNA–drug complexes were measured on a Shimadzu Pharmaspec 1700 unit (Shimadzu Corporation, Kyoto, Japan) equipped with the Peltier controlled TMSPC-8 model accessory and a temperature programmer as described earlier [26]. In a typical experiment, the DNA sample (~50 μM) was mixed with different concentrations of the drug under study in degassed buffer and the mixture was heated at a rate of 60 $K \cdot h^{-1}$, continuously recording the absorbance change at 260 nm. The melting temperature (T_{fus}) is the midpoint of the hyperchromic transition as determined by the maxima of the first derivative plots.

2.5. Differential scanning calorimetry

Excess heat capacities as a function of temperature were measured on a Microcal VP-differential scanning calorimeter (DSC) (MicroCal, Inc., Northampton, MA, USA) as described previously [26]. In a series of DSC scans, both the cells were loaded at first with the buffer, equilibrated at $T = 293.15$ K for 15 min, and scanned from 293.15 K to 393.15 K at the rate of 60 $K \cdot h^{-1}$. The buffer scans were repeated till the base line was reproducible (noise specification <2.1 $\mu J \cdot K^{-1}$ and repeatability specification <5.46 $\mu J \cdot K^{-1}$). Typically about 8 to 10 scans were required to achieve reproducibility. On the cooling cycle, the sample cell was rinsed, loaded with the DNA followed by the DNA–drug complex (molar ratio = 0.8), and scanned in the same temperature range. Each experiment was repeated twice with separate fillings. The DSC thermograms of excess heat capacity versus temperature were analyzed using the Origin 7.0 software. The area under the experimental heat capacity (ΔC_p°) curves were used to determine the calorimetric transition enthalpy (ΔH_{cal}) given by the equation $H_{cal} = \int C_p^\circ dT$, where T refers to the absolute scale temperature. This calorimetrically determined enthalpy is model-independent and thus unrelated to the nature of the transition. The temperature at which excess heat capacity is at a maximum defines the transition temperature (T_{fus}). The model-dependent van't Hoff enthalpy (ΔH_v) was obtained by shape analysis of the calorimetric data, and the cooperativity factor was obtained from the ratio ($\Delta H_{cal}/\Delta H_v$).

2.6. Isothermal titration calorimetry

Isothermal titration calorimetry (ITC) experiments were performed on a VP ITC unit (MicroCal). Titrations were performed at four temperatures *viz.* (283.15, 293.15, 303.15, and 313.15) K as described in details elsewhere [27]. DNA and drug solutions were degassed on the MicroCal's Thermovac unit before loading to avoid the formation of bubbles in the calorimeter cell. The instrument control, titration and analysis were performed using the dedicated Origin 7.0 software provided with the unit. Titrations were performed by injecting the DNA solution from the syringe into the drug solution kept in the calorimeter cell. The duration of each injection was 10 s and the delay time between each injection was 240 s. The initial delay before the first injection was 60 s. Corresponding control experiments to determine the heat of dilution of the DNA were performed by injecting identical volumes of the same concentration of the DNA into the buffer. The heat of dilution of injecting the buffer into each of the drug solution was measured to be negligible. Each injection generated a heat burst curve (micro Joule per second *versus* time). The resulting thermograms after appropriate corrections were analyzed using single set of binding sites model of Levenberg–Marquardt non-linear least squares curve fitting algorithm, inbuilt with the software of the unit. The association constant K_a, stoichiometry N, and molar heat of binding ΔH° were obtained using the following relation:

$$K_a = \frac{\theta}{(1-\theta)[X]}, \tag{1}$$

where θ = fraction of sites occupied by drug X, and [X] = concentration of free drug. Therefore, the total concentration of drug (free and bound), X_t is given by

$$X_t = [X] + n\theta M_t, \tag{2}$$

where M_t is the bulk concentration of macromolecule in the active cell volume V_{cell}. The total heat content Q of the solution in the active cell volume is

$$Q = n\theta M_t \Delta H^\circ V_{cell}. \tag{3}$$

Considering the volume change ΔV_i accompanying the injection i, the heat released, ΔQ_i from the ith injection is

$$\Delta Q_i = Q_i + \frac{\Delta V_i}{V_{cell}}\left[\frac{Q_i + Q_{(i-1)}}{2}\right] - Q_{(i-1)}. \tag{4}$$

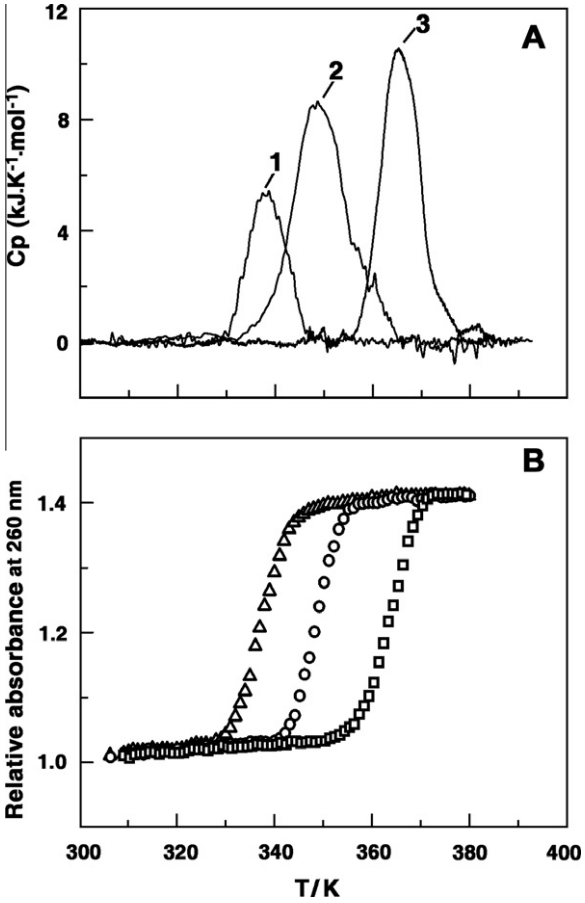

FIGURE 2. (A) DSC thermograms of HT DNA (curve 1), ADG-HT DNA complex (curve 2) and DAU-HT DNA complex (curve 3). (B) Thermal melting profile of HT DNA (△), ADG-HT DNA complex (○), and DAU-HT DNA complex (□).

Binding Gibbs energy and entropy change were obtained using the relation

$$\Delta G^{\circ} = -RT \ln K_a = \Delta H^{\circ} - T\Delta S^{\circ} \quad (5)$$

where R signifies the universal gas constant ($8.314\ \mathrm{J \cdot K^{-1} \cdot mol^{-1}}$). Specific heat capacity changes (ΔC_p°) were derived from the plots of enthalpy (ΔH°), *versus* temperature (T), at constant pressure, using the following relation

$$\Delta C_p^{\circ} = [\partial(\Delta H^{\circ})/\partial T]_p. \quad (6)$$

The ITC unit was periodically calibrated electrically and verified with water–water dilution experiments as per criteria of the manufacturer that the mean energy per injection was <5.46 μJ and standard deviation was <0.063 μJ.

3. Results and discussion

3.1. Differential scanning calorimetry and optical thermal melting studies, and evaluation of apparent binding affinity

Effective intercalator small molecules are known to enhance the stability of the DNA helix and this in turn results in an enhancement of the melting temperature (T_{fus}) that is revealed from optical melting and differential scanning calorimetry experiments. Although increase in melting temperature cannot be directly correlated with binding affinity, high ΔT_{fus} values are generally suggestive of strong interactions. The effect of ADG and DAU on the thermal stability of DNA was at first investigated from DSC experiments. HT DNA under the present experimental conditions denatured with a single endothermic peak with melting temperature (T_{fus}°) of 338.40 K (figure 2A). Binding ADG and DAU induced stability to the helical structure and the thermal melting temperature was enhanced. Enhancement of the melting temperatures by 10.2 K and 28.0 K, respectively, with ADG and DAU under saturating conditions indicated that the binding stabilized the DNA structure considerably. The melting temperatures are presented in table 1. It can be seen that a remarkably higher stabilization was effected by DAU compared to ADG. Another important aspect is the cooperativity of the transition and the ratio between the calorimetry enthalpy (ΔH_{cal}) and van't Hoff enthalpy (ΔH_{vH}) that gives quantitative information on the cooperativity. The ratio is an index of the mean cooperative unit size for cooperative transitions. For DNA alone the ratio was 5.1 and is close to that reported in the literature [28]. The ratio of $\Delta H_{vH}/\Delta H_{cal} > 1$ is related to the mean number of base pairs that melt as a single thermodynamic entity, and may denote significantly populated intermediate states [29,30]. For the drug bound systems studied here, there were significant differences between the calorimetric and van't Hoff enthalpies presented in table 1. Here we find that in presence of the drugs the ratio is lower as compared to the DNA alone, without significant change in the shape of the curve (figure 2A). Therefore it can be concluded that the denaturation process is not altered but shifted to higher temperatures only. Furthermore, since there is no broadening of the peaks, it appears that there is no migration of the bound drugs to unmelted regions when the low melting AT regions of the DNA duplex are melted. In all the cases, including for DNA alone, the denaturation process was irreversible.

The DSC results were also substantiated from optical melting studies. In absorbance, cooperative melting transition with ~40% hyperchromicity and without any hysterisis were observed for the DNA and the drug complexes. The UV melting profiles of HT DNA and its complexes at saturation D/P (drug/DNA base pair molar ratio) values are presented in figure 2B. The T_{fus}° values were (338.4, 348.5, and 365.5) K, respectively, for free DNA, ADG complex ($D/P = 0.8$) and DAU complex ($D/P = 0.8$). The data from optical melting are in excellent agreement to those obtained from DSC studies. The helix stabilization data of DNA by these drugs from optical melting are also presented in table 1.

TABLE 1
Differential scanning calorimetry and optical melting results of ADG and DAU binding to HT DNA.[a]

DNA	Mass fraction purity	T_{fus}°/K (DSC)	T_{fus}°/K (optical melting)	ΔT_{fus}	ΔH_{cal}/ (kJ · mol^{-1})	ΔH_{vH}/ (kJ · mol^{-1})	ΔH_{vH}/ ΔH_{cal}	$10^5\ KT_{fus}$/M^{-1}	$10^5\ K_{obs}$/M^{-1}
No drug		338.05 ± 0.05	338.40 ± 0.10		60.9 ± 0.1	310.4 ± 0.5	5.1 ± 0.2		
ADG	0.99	348.30 ± 0.05	348.50 ± 0.10	10.20 ± 0.15	90.7 ± 0.1	341.2 ± 0.8	3.8 ± 0.1	0.94 ± 0.02	6.67 ± 0.05
DAU	0.90	366.05 ± 0.06	365.50 ± 0.30	27.55 ± 0.04	105.0 ± 0.2	496.0 ± 0.6	4.7 ± 0.1	9.75 ± 0.15	53.0 ± 0.40

[a] Melting temperature of free DNA (T_{fus}°) and in the presence of saturating amounts of drug (T_{fus}). ΔH_{cal} and ΔH_{vH} represent the calorimetric and vant' Hoff enthalpy, respectively. KT_{fus} is the drug-binding constant at T_{fus} and K_{obs} is the drug-binding constant at $T = 293.15$ K. The data presented are averages of four determinations. Experiments were done in 20 mM CP buffer, pH 7.01.

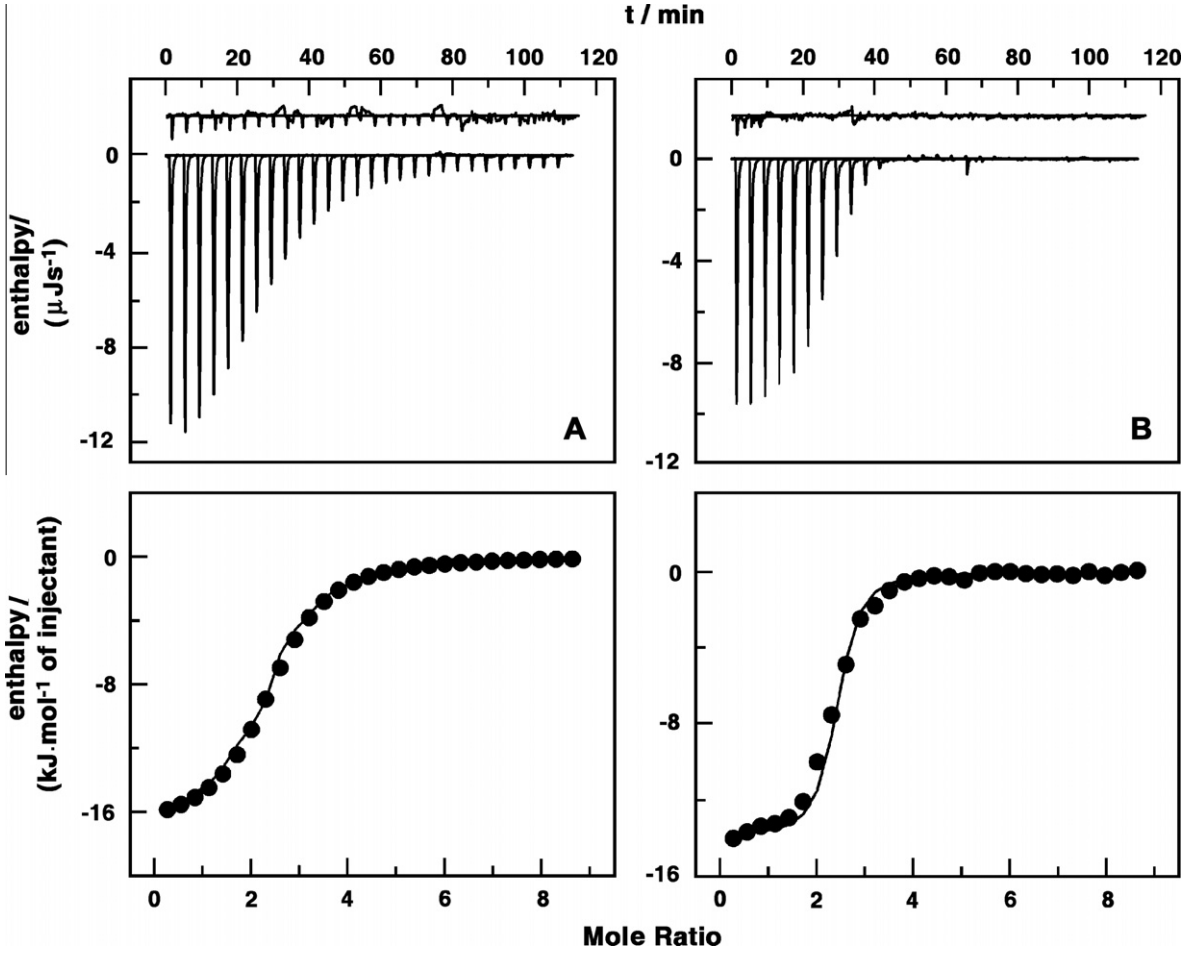

FIGURE 3. ITC binding profiles for the binding of (A) ADG and (B) DAU to HT DNA at $T = 293.15$ K. The top panels represent the raw data for the sequential injection of HT DNA into the drugs, and the bottom panels show the integrated heat data after correction of heat of dilution against the molar ratio of DNA/[drug]. The data points were fitted to one site model, and the solid lines represent the best-fit data.

Melting temperature data were used to calculate the binding constant of the association using the following equation [31]

$$1/T^{\circ}_{\mathrm{fus}} - 1/T_{\mathrm{fus}} = (R/n\Delta H_{\mathrm{wc}}) \ln(1 + K_{T_{\mathrm{fus}}}\alpha) \quad (7)$$

where T°_{fus} is the optical melting temperature of the DNAs in the absence of the drug, T_{fus} is the melting temperature in presence of saturating amounts of the drugs, ΔH_{wc} is the enthalpy of DNA melting, R is the universal gas constant ($8.314\,\mathrm{J \cdot K^{-1} \cdot mol^{-1}}$), $K_{T_{\mathrm{fus}}}$ is the drug binding constant at the T_{fus}, α is the free drug activity, that may be estimated by one half of the total drug concentration, and n is the site size of the drug binding. The calculated apparent binding constant at the melting temperature can be extrapolated to a reference temperature (say 293.15 K) using the standard relationship,

$$\delta[\ln(K_{\mathrm{obs}})]/\delta(1/T) = -(\Delta H_b/R), \quad (8)$$

where K_{obs} is the drug binding constant at the reference temperature T and ΔH_b, the binding enthalpy which was directly determined from the isothermal titration calorimetry experiment (*vide infra*). The binding constant (K_{obs}) calculated at $T = 293.15$ K from these data are depicted in table 1. It can be observed that the K_{obs}

TABLE 2
Salt dependent isothermal titration calorimetric data for the binding of ADG and DAU to DNA at 293.15 K.[a]

Drug	[Na^+] Molarity/mM	$10^{-5}K_a/M^{-1}$	N	$\Delta G^{\circ}/(\mathrm{kJ \cdot mol^{-1}})$	$\Delta H^{\circ}/(\mathrm{kJ \cdot mol^{-1}})$	$T\Delta S^{\circ}/(\mathrm{kJ \cdot mol^{-1}})$	$\Delta G^{\circ}_t/(\mathrm{kJ \cdot mol^{-1}})$	$\Delta G^{\circ}_{\mathrm{pe}}/(\mathrm{kJ \cdot mol^{-1}})$	$Z\Psi$
ADG	10	5.00 ± 0.04	0.44 ± 0.02	−32.30 ± 0.14	−46.20 ± 0.20	−14.24	−24.95 ± 0.12	−7.35 ± 0.10	−0.65 ± 0.05
	20	3.00 ± 0.05	0.43 ± 0.01	−31.04 ± 0.50	−43.26 ± 0.14	−12.18	−24.78 ± 0.42	−6.26 ± 0.15	
	50	1.67 ± 0.10	0.41 ± 0.01	−29.61 ± 0.35	−37.93 ± 0.63	−8.44	−24.82 ± 0.36	−4.79 ± 0.23	
	100	1.11 ± 0.04	0.40 ± 0.02	−28.60 ± 0.25	−33.73 ± 0.22	−5.30	−24.91 ± 0.22	−3.70 ± 0.18	
DAU	10	30.0 ± 0.50	0.45 ± 0.02	−36.71 ± 0.48	−36.54 ± 0.35	−0.04	−27.30 ± 0.15	−9.41 ± 0.25	0.83 ± 0.20
	20	20.0 ± 0.30	0.43 ± 0.01	−35.70 ± 0.05	−33.60 ± 0.50	1.89	−27.72 ± 0.26	−7.98 ± 0.20	
	50	7.97 ± 0.08	0.40 ± 0.03	−33.43 ± 0.24	−31.50 ± 0.22	1.60	−27.34 ± 0.50	−6.13 ± 0.18	
	100	4.73 ± 0.02	0.40 ± 0.02	−32.16 ± 0.30	−29.82 ± 0.28	2.18	−27.47 ± 0.33	−4.60 ± 0.20	

[a] All the data in this table are derived from ITC experiments conducted in CP buffer of (10, 20, 50, and 100) mM [Na^+], pH 7.01 and are average of four determinations. K_a the affinity and ΔH°, the enthalpy change was determined from ITC profiles fitting to Origin 7 software as described in the text. N is the binding stoichiometry. T is the temperature at which the experiment was performed. The values of ΔG°, the Gibbs free energy change and $T\Delta S^{\circ}$, the entropy contribution were determined using the equations $\Delta G^{\circ} = -RT\ln K_a$, and $T\Delta S^{\circ} = \Delta H^{\circ} - \Delta G^{\circ}$. Here ΔG°_t and $\Delta G^{\circ}_{\mathrm{pe}}$ represent non-polyelectrolytic and polyelectrolytic contribution to the Gibbs free energy. All the ITC profiles were fit to a model of single binding sites.

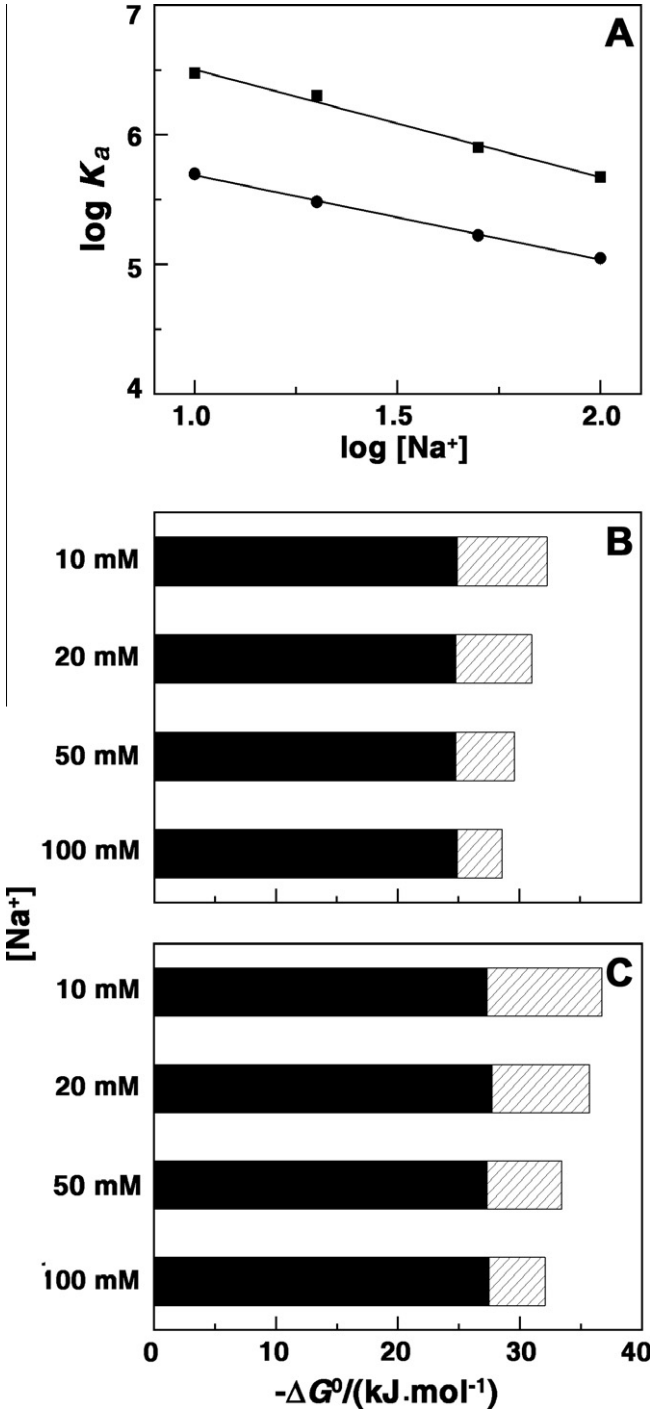

FIGURE 4. (A) Log–log plot of variation of the intrinsic binding Ka as a function of ionic strength [Na^+] for the complexation of ADG (●) and DAU (■) with HT DNA. Nonpolyelectrolytic (black) (ΔG_t°) and polyelectrolytic (shaded) (ΔG_{pe}°) contribution of binding of (B) ADG and (C) DAU with HT DNA.

value for DNA–DAU complex was one order higher than that of DNA–ADG complex.

3.2. Isothermal titration calorimetry of drug–DNA interaction

To understand the thermodynamics of the interaction of the two drugs with DNA, detailed thermodynamic data were derived from high sensitive isothermal titration calorimetric studies. ITC measurements provide detailed information [32,33] on thermodynamic quantities like enthalpy of binding, the entropy contribution to the binding and also the affinity and stoichiometry of the interaction. In figure 3A and B, representative calorimetric profiles of the titration of ADG and DAU to DNA at T = 293.15 K are presented. The binding is an exothermic process and has a single binding event in both cases. Exothermic binding of daunomycin to DNA and polynucleotides has been reported by Chaires also [18,25]. The heat liberated in each injection was corrected for the heat of dilution that was determined in a separate but identical experiment injecting DNA into buffer alone. The resulting values were plotted against the molar ratio of drug/DNA and fitted to a one site model by nonlinear least square method (curves in the lower panel). The equilibrium constant, binding stoichiometry, enthalpy change, entropy contribution, and the Gibbs free energy change obtained from the calorimetric data are summarized in table 2. The binding constants (K_a) of ADG and DAU to DNA were evaluated to be $3.00 \cdot 10^5\ M^{-1}$ and $2.00 \cdot 10^6\ M^{-1}$, respectively. A remarkably stronger binding of the DAU over ADG is thus apparent from the calorimetric data as well. An N value of around 0.43 in both cases indicates that the binding spans about 2 to 3 base pairs of DNA. The thermodynamic parameters of the interaction, however, were significantly different. The Gibbs free energy change for ADG was about $-31.04\ kJ \cdot mol^{-1}$ while for DAU it was higher by $4.66\ kJ \cdot mol^{-1}$ at $-35.70\ kJ \cdot mol^{-1}$. The later value is close to the value reported by Suh *et al.* [25]. The binding of ADG was favoured by large negative enthalpy and an unfavorable entropy term of $-12.18\ kJ \cdot mol^{-1}$. For DAU also the binding was enthalpy driven with a small entropy factor. Clearly, it appears that the thermodynamics of the interaction are grossly different like the entropy was unfavourable in ADG while the same, although small, was favourable in the case of DAU. To analyze the interaction in more details we performed salt and temperature dependent calorimetry experiments.

3.3. Salt dependent isothermal titration calorimetry studies

Previously published spectroscopic data by Maiti and colleagues have suggested that electrostatic interactions are important for the binding of ADG to DNA. This was based on the presumption that ADG may exist as a monovalent cation in the presence of DNA [22]. On the other hand, for DAU, the daunosamine moiety is positively charged and Chaires and colleagues have revealed that the polyelectrolytic contribution to the binding free energy is significant as evidenced from the results of partitioning the Gibbs free energy between polyelectrolytic and nonpolyelectrolytic components [5,34]. On a comparative basis, we studied the effect of salt concentration in the range of [Na^+] 10 mM to 100 mM on the binding of ADG and DAU to HT DNA by calorimetric experiments in conjunction with van't Hoff analysis. As the [Na^+] concentration was increased from 10 mM to 100 mM [Na^+], the binding affinity of the interaction decreased in both cases. For ADG the decrease in K_a was from $5.0 \cdot 10^5\ M^{-1}$ to $1.11 \cdot 10^5\ M^{-1}$ while for DAU a higher fall from $3.00 \cdot 10^6\ M^{-1}$ at 10 mM to $4.73 \cdot 10^5\ M^{-1}$ at 100 mM occurred (table 2). The decrease in the binding affinity was thus more pronounced for DAU compared to ADG and this has been well documented in the literature from the studies of Chaires and colleagues as well [5,34]. The binding of both ADG and DAU are thus thermodynamically linked to Na^+ concentration. Although there was not much change in the free energy change in the 10 mM to 100 mM [Na^+], the variation of the other thermodynamic parameters were remarkably different for ADG and DAU. For ADG, ΔH° became less negative (from $-46.20\ kJ \cdot mol^{-1}$ to $-33.73\ kJ \cdot mol^{-1}$) and the unfavourable entropy contribution decreased from $-14.24\ kJ \cdot mol^{-1}$ to $-5.30\ kJ \cdot mol^{-1}$. On the other hand, for DAU, ΔH° values varied from $-36.54\ kJ \cdot mol^{-1}$ to

TABLE 3
Temperature dependent isothermal titration calorimetric data for the binding of ADG and DAU to DNA.[a]

Drug	T/K	$10^{-5}K_a/M^{-1}$	N	ΔG°/(kJ · mol^{-1})	ΔH°/(kJ · mol^{-1})	$T\Delta S^\circ$/(kJ · mol^{-1})	ΔC_p° /(kJ · mol^{-1})	ΔG°_{hyd} /(kJ · mol^{-1})
ADG	283.15	6.00 ± 0.15	0.52 ± 0.03	−31.46 ± 0.05	−33.60 ± 0.05	−2.14	−0.64 ± 0.01	−51.44 ± 0.05
	293.15	3.00 ± 0.20	0.43 ± 0.05	−30.91 ± 0.10	−43.26 ± 0.08	−12.18		
	303.15	0.62 ± 0.05	0.42 ± 0.02	−27.93 ± 0.08	−46.62 ± 0.20	−18.82		
	313.15	0.48 ± 0.03	0.40 ± 0.02	−27.97 ± 0.05	−53.76 ± 0.30	−25.8		
DAU	283.15	40.0 ± 0.50	0.54 ± 0.03	−37.38 ± 0.05	−27.43 ± 0.08	+10.29	−0.68 ± 0.01	−54.80 ± 0.06
	293.15	20.0 ± 0.88	0.43 ± 0.01	−35.70 ± 0.08	−33.60 ± 0.28	+1.89		
	303.15	9.00 ± 0.20	0.38 ± 0.01	−31.80 ± 0.10	−41.16 ± 0.08	−9.37		
	313.15	8.0 ± 0.35	0.32 ± 0.02	−35.7 ± 0.05	−47.46 ± 0.20	−11.93		

[a] All the data in this table are derived from ITC experiments conducted in 20 mM CP buffer pH 7.01 and are average of four determinations. T is the temperature at which the experiment was performed. K_a and ΔH° values were determined from ITC profiles fitting to Origin 7.0 software. The values of ΔG° and $T\Delta S^\circ$ were determined using the equations $\Delta G^\circ = -RT\ln K_a$ and $T\Delta S^\circ = \Delta H^\circ - \Delta G^\circ$. N is the binding stoichiometry. All the ITC profiles were fit to a model of single binding site.

-29.82 kJ · mol^{-1} while $T\Delta S^\circ$ contribution became more favourable but still remained insignificant.

Polyelectrolytic theories based on Manning's counter ions condensation model describe the process and provide a basis for interpreting the above data [35]. From polyelectrolytic theory, the slope of the best fit line for a plot of $\lg K_a$ *versus* $\lg[Na^+]$ is related to the counter-ion release [36] by the following relation

$$SK = \delta \lg(K_a)/\delta \lg([Na^+]) = -Z_\Psi, \quad (9)$$

where SK is equivalent to the number of counter ions released upon binding of a drug, Z is the apparent charge of the bound ligand per phosphate binding and Ψ is the fraction of $[Na^+]$ bound per phosphate group. The slope of the plot of $\lg K_a$ *versus* $\lg[Na^+]$ (figure 4A) gave values of -0.65 and -0.83, respectively, for ADG and DAU. The values of $Z\Psi$ reported for daunomycin–DNA complexes are in the range 0.84 to 1.08 [5,18]. These values represent the counter ions released per phosphate upon binding and suggest stronger electrostatic contact of DAU over ADG with DNA. This has been further verified by dissecting the observed binding Gibbs free energy by partitioning to electrostatic (ΔG°_{pe}) and non-electrostatic (ΔG°_t) contributions.

The polyelectrolytic contribution to the overall observed Gibbs free energy can be quantitatively estimated from the relationship

$$\Delta G^\circ_{pe}| = -Z\Psi RT\ln([Na^+]) \quad (10)$$

at a given salt concentration and the non-electrostatic contribution can be calculated as the difference between ΔG° and ΔG°_{pe}. Here $Z\Psi$ is the slope of the van't Hoff plot (see above). At 10 mM $[Na^+]$, the contribution of ΔG°_{pe} has been determined to be -7.35 kJ · mol^{-1} and -9.41 kJ · mol^{-1}, respectively, for ADG and DAU. These are about 23% and 26%, respectively, of the total Gibbs free energy change. At 100 mM of $[Na^+]$, the values of ΔG°_{pe} have been estimated to be -3.7 kJ · mol^{-1} and -4.6 kJ · mol^{-1} for ADG and DAU, respectively. These are about 13% and 15% of the total Gibbs free energy change. A higher polyelectrolytic contribution was revealed for DAU compared to ADG. For charged intercalators, it has been reported by Chaires that the value of ΔG°_{pe} is salt dependent and may vary from 0 kJ · mol^{-1} to -16.8 kJ · mol^{-1} [37]. Even uncharged intercalators are suggested to have polyelectrolytic contributions due to separation of phosphates that reduces the extent of counter ions' condensation that releases cations [38,39]. A graphical representation of the partitioned Gibbs free energy is presented in figure 4B and C. It can be observed that in both cases the ΔG°_{pe} contribution decreased on increasing the [Na+] concentration. Although ΔG°_t has major role in stabilizing the intercalative complexes of both ADG and DAU, the role of electrostatic forces are significant particularly in the case of ADG which is not charged. Studies reported here also reiterate the involvement of major contribution from non-polyelectrolytic forces in the binding. In the case of ADG, it has been suggested that a weak transient positive charge may be developed at the N6 position in the presence of nucleic acids [22]. It is likely that such transient charge development may be the cause of the significant electrostatic contribution to its DNA binding observed here. Clearly, the electrostatic contributions to the binding of DAU to DNA are higher than those of ADG and in both cases non electrostatic contribution is much higher over polyelectrolytic contribution.

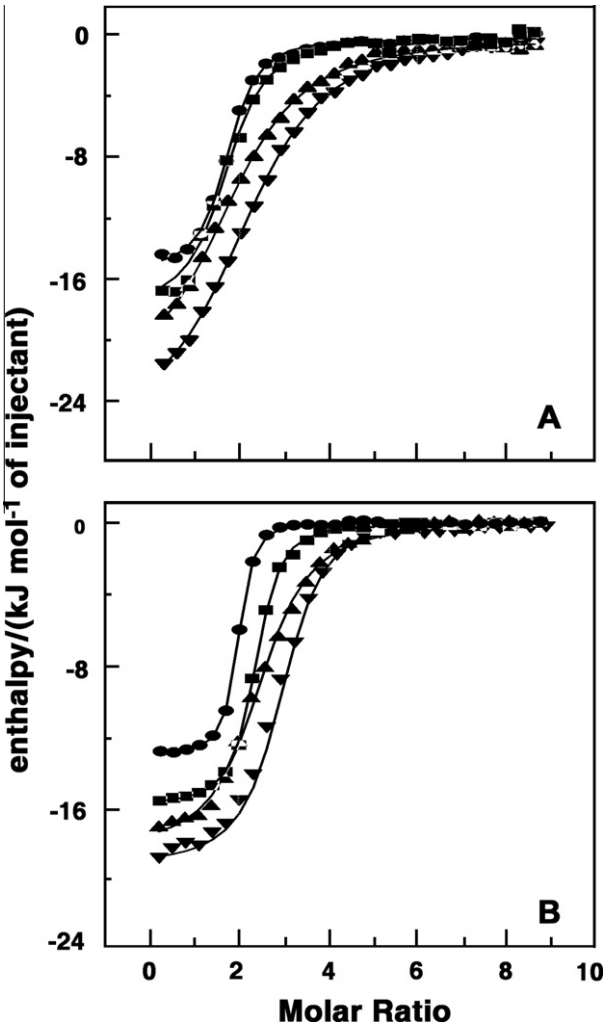

FIGURE 5. Plot of enthalpy against mole ratio to show the integrated heat results of (A) ADG and (B) DAU titration to HT DNA after correction of heat of dilution against mole ratio of DNA/drug at T = 283.15 K (●), 293.15 K (■), 303.15 K (▲) and 313.15 K (▼) temperature respectively. The results were fitted to a one-site model and the solid lines represent the best-fit.

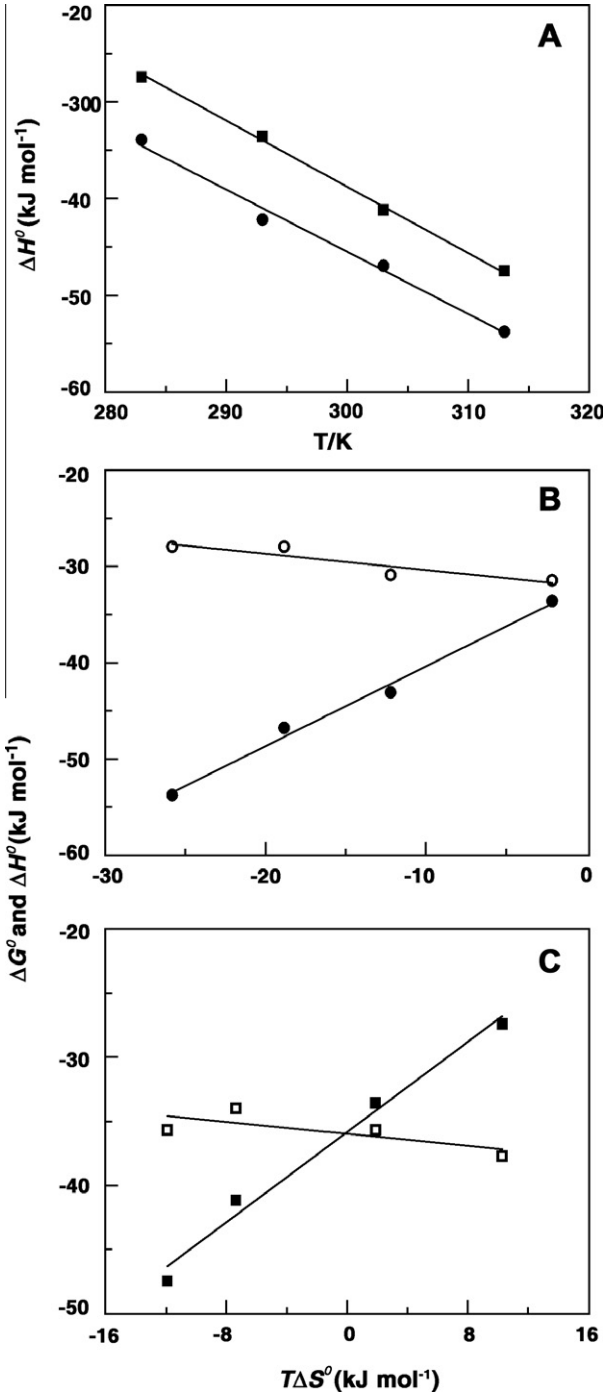

FIGURE 6. (A) Plot of variation of enthalpy of binding (ΔH°) with temperature for the binding of ADG (●) and DAU (■) with HT DNA. Plot of ΔG° (○, □) and ΔH° (●, ■) *versus* $T\Delta S^\circ$ for the binding of (B) ADG and (C) DAU with HT DNA, respectively.

3.4. Temperature dependent isothermal titration calorimetry

To obtain insight about the driving forces of interaction of these drugs with DNA, complex formation was examined as a function of temperature over the range 283.15 K to 313.15 K. No variation in pH of these solutions was observed in the temperature range studied here. The binding isotherms observed at different temperatures were sigmoidal. Comparison of the ITC data (table 3) in terms of the fitted curves is shown in figure 5. Overall, as the temperature increased, the affinity values decreased the binding enthalpies became more negative with their magnitudes increasing. The negative enthalpy of binding at all temperatures indicated favourable exothermic binding interaction. In both cases the entropy contribution became more and more unfavourable with temperature and the reaction seems to be driven by enthalpy at all temperatures. The energetics of the interaction indicated significant differences in the molecular forces that contribute and control the binding of ADG and DAU to DNA.

Variation of the enthalpy change with temperature can provide information on the heat capacity changes (ΔC_p°) of the binding. The observed enthalpy change (ΔH°) varied linearly on the experimental temperature in the range for both ADG and DAU (figure 6A) indicating that there is no measurable shift in the pre-existing equilibrium between the conformational states of DNA in the temperature range studied. Strong enthalpy–entropy compensation was, however, observed making Gibbs free energy of binding nearly independent of temperature (figure 6B and C). The heat capacity values obtained from figure 6A yielded values of -0.643 and $-0.680\ \text{kJ}\cdot\text{mol}^{-1}\cdot\text{K}^{-1}$, respectively, for the binding of ADG and DAU. A ΔC_p° value of $-0.672\ \text{kJ}\cdot\text{mol}^{-1}\cdot\text{K}^{-1}$ has been reported for daunomycin–CT DNA interaction by Chaires [5,40]. The negative values of ΔC_p° in both cases suggest that the binding is specific and accompanied by burial of non-polar surface area [40–42].

The $\Delta G^\circ_{\text{hyd}}$ Gibbs free energy contribution for the hydrophobic transfer step for the binding of drug to DNA has been calculated from the relationship, $\Delta G^\circ_{\text{hyd}} = (80 \pm 10)\ \text{kJ}\cdot\text{mol}^{-1}$, the ΔC_p° described by Record and colleagues [43]. The values of $\Delta G^\circ_{\text{hyd}}$ for ADG and DAU binding to HT DNA were found to be $-51.44\ \text{kJ}\cdot\text{mol}^{-1}$ and $-54.80\ \text{kJ}\cdot\text{mol}^{-1}$, respectively (table 3). These values lie well within the range that was observed frequently for DNA and RNA intercalators [26,40,42]. It is likely that the thermodynamic components of interaction like the water uptake, water release, *etc.* may be significantly similar and this may be the cause for the similarities reflected in the $\Delta G^\circ_{\text{hyd}}$ values.

4. Conclusions

Here we present experiments to understand the energetics of the DNA binding of two sugar containing molecules ADG and DAU. The binding parameters evaluated from thermal melting and calorimetry experiments revealed that DAU showed an almost one order higher DNA binding affinity compared to ADG. Compared to ADG, DAU has different functional groups in the molecule: the four fused intercalator rings, the anchoring ring and the anchoring function with H-bonding capability, and the charged amino sugar are all additional DNA binding functions in DAU. Furthermore, the geometry of the aromatic ring system in daunomycin namely the aglycone chromophore and the chromophore of ADG are different and the same for DAU is more base pair homologous and this may contribute to better intercalation geometry for DAU compared to ADG. Thermodynamic parameters suggested that the binding in both cases was enthalpy driven but the entropy contributions are different, being unfavourable in ADG and favourable in DAU. The electrostatic contribution to the binding of DAU to DNA was higher than that of ADG although non electrostatic contribution was much higher over polyelectrolytic contribution in both cases. The binding was also characterized by strong enthalpy–entropy compensation in both cases but the different ΔC_p° values suggested different interacting forces in the complexation of these two compounds with DNA.

Acknowledgements

The authors are grateful to Dr. Basudeb Achari, Ex. Scientist of the Chemistry Division of Indian Institute of Chemical Biology for the gift of the sample of aristololactam-β-D-glucoside. A. Das is a

NET Senior Research Fellow of Council of Scientific and Industrial Research (CSIR). Partial financial assistance for this work through grants from the net work project NWP0036 entitled "*Comparative genomics and biology of non coding RNA in the human genome*" (CSIR), Govt. of India is gratefully acknowledged. The authors thank all the colleagues of the Biophysical Chemistry Laboratory, CSIR – Indian Institute of Chemical Biology for their help and cooperation at every stage of this work. We appreciate the critical comments of the anonymous reviewer that enabled us to improve the manuscript.

References

[1] M.J. Waring, L.P.G. Wakelin, Nature 252 (1974) 653–657.
[2] M.J. Waring, Annu. Rev. Biochem. 50 (1981) 159–192.
[3] J.B. Chaires, Curr. Opin. Struct. Biol. 8 (1998) 314–320.
[4] R. Martínez, L. Chacón-García, Curr. Med. Chem. 12 (2005) 127–151.
[5] J.B. Chaires, Biopolymers 44 (1997) 201–215.
[6] J.B. Chaires, Annu. Rev. Biophys. 37 (2008) 135–151.
[7] Z. Chen, D. Zhu, in: Brossi (Ed.), The Alkaloids, vol. 31, Academic Press, Orlando, 1987, p. 29.
[8] J.M. Cassady, W.M. Baird, C.J. Chang, J. Nat. Prod. 53 (1990) 23–41.
[9] L. Gianni, B.C. Corden, C.E. Meyer, Rev. Biochem. Toxicol. 5 (1982) 1–82.
[10] J.B. Chaires, K.R. Fox, J.E. Herrera, M. Britt, M.J. Waring, Biochemistry 26 (1987) 8227–8236.
[11] R.B. Weiss, Semin. Oncol. 19 (1992) 670–686.
[12] A. Rabbani, S. Abdosamadi, N. Sari-Saraf, Acta Pharmacol. Sin. 28 (2007) 731–737.
[13] F. Zunino, R. Gambetta, A. Di Marco, F. Zaccara, Biochim. Biophys. Acta 277 (1972) 489–498.
[14] A. Marco, F. Arcamone, Arzneim. Forsch. 25 (1975) 368–374.
[15] K.X. Chen, N. Gresh, B. Pullman, Mol. Pharmacol. 30 (1986) 279–286.
[16] D. Gaál, F. Hudecz, Eur. J. Cancer 34 (1998) 155–161.
[17] S. Chakraborty, R. Nandi, M. Maiti, B. Achari, C.R. Saha, S.C. Pakrashi, Biochem. Pharmacol. 38 (1989) 3683–3687.
[18] J.B. Chaires, Biophys. Chem. 35 (1990) 191–202.
[19] R. Nandi, S. Chakraborty, M. Maiti, Biochemistry 30 (1991) 3715–3720.
[20] J.B. Chaires, S. Satyanarayana, D. Suh, I. Fokt, T. Przewolka, W. Priebe, Biochemistry 35 (1996) 2047–2053.
[21] M. Trieb, C. Rauch, B. Wellenzohn, F. Wibowo, T. Loerting, E. Mayer, K.R. Liedl, J. Biomol. Struct. Dyn. 21 (2004) 713–724.
[22] S. Chakraborty, R. Nandi, M. Maiti, Biochem. Pharmacol. 39 (1990) 1181–1186.
[23] S.C. Pakrashi, P. Ghosh-Dastidar, S. Basu, B. Achari, Phytochemistry 16 (1977) 1103–1104.
[24] B. Achari, S. Bandyopadhyay, A.K. Chakraborty, S.C. Pakrashi, Org. Mag. Reson. 22 (1984) 741–746.
[25] D. Suh, Y.K. Oh, M.W. Hur, B. Ahn, J.B. Chaires, Nucleos. Nucleot. Nucl. Acids 21 (2002) 637–649.
[26] M.M. Islam, R. Sinha, G. Suresh Kumar, Biophys. Chem. 125 (2007) 508–520.
[27] M.M. Islam, P. Pandya, S.R. Chowdhury, S. Kumar, G. Suresh Kumar, J. Mol. Struct. 891 (2008) 498–507.
[28] H.K.S. Souza, Thermochim. Acta 501 (2010) 1–7.
[29] D. Esposito, P. Del Vecchio, G. Barone, J. Am. Chem. Soc. 119 (1997) 2606–2613.
[30] L. Petraccone, S. Baiano, G. Fiorentino, G. Barone, C. Giancola, Thermochim. Acta 418 (2004) 47–52.
[31] D.M. Crothers, Biopolymers 10 (1971) 2147–2160.
[32] A.L. Faig, Biopolymers 87 (2007) 293–301.
[33] N.J. Buurma, I. Haq, Methods 42 (2007) 162–172.
[34] J.B. Chaires, Biopolymers 24 (1985) 403–419.
[35] G.S. Manning, Physica A 231 (1996) 236–253.
[36] M.T. Record Jr., C.F. Anderson, T.M.Q. Lohman, Rev. Biophys. 11 (1978) 103–178.
[37] J.B. Chaires, Anti-Cancer Drug Des. 11 (1996) 569–580.
[38] W.D. Wilson, I.G. Lopp, Biopolymers 18 (1979) 3025–3041.
[39] R.A. Friedman, G.S. Manning, Bipolymers 23 (1984) 2671–2712.
[40] J. Ren, T.C. Jenkins, J.B. Chaires, Biochemistry 39 (2000) 8439–8447.
[41] K.L. Buchmueller, S.L. Bailey, D.A. Matthews, Z.T. Taherbhai, J.K. Register, Z.S. Davis, C.D. Bruce, C. O'Hare, J.A. Hartley, M. Lee, Biochemistry 45 (2006) 13551–13565.
[42] K.M. Guthrie, A.D.C. Parenty, L.V. Smith, L. Cronin, A. Cooper, Biophys. Chem. 126 (2007) 117–123.
[43] J.H. Ha, R.S. Soplar, M.T. Record Jr., J. Mol. Biol. 209 (1989) 801–881.

JCT-12-227